Thermoreversible Gelation of Aqueous Methylcellulose Solutions

Kazuto Kobayashi,[†] Ching-i Huang,[§,‡] and Timothy P. Lodge*[§]

Department of Chemistry and Department of Chemical Engineering & Materials Science, University of Minnesota, Minneapolis, Minnesota 55455-0431

Received February 19, 1999; Revised Manuscript Received August 16, 1999

ABSTRACT: The thermoreversible gelation of methylcellulose in aqueous solution has been studied by static and dynamic light scattering (DLS), small-angle neutron scattering (SANS), and rheology. At 20 °C, dilute solution light scattering establishes the molecular weight, second virial coefficient, radius of gyration, and hydrodynamic radius of the polymer. Semidilute solutions exhibit two relaxation modes in DLS, one reflecting cooperative diffusion and the other attributable to pregel clusters. Rheological measurements in this regime also suggest a weak supermolecular association. The gelation of semidilute solutions proceeds in two stages with increasing temperature above 20 °C, consistent with previous reports. The first stage is attributable to clustering of chains, driven by hydrophobic association, and extends up to approximately 50 °C. This process is accompanied by an increase in the low-frequency dynamic elastic modulus, G', and an increase in both light and neutron scattered intensity. The DLS properties of these solutions, and the angular dependence of the scattered intensity, is not greatly affected by this association. The second stage of gelation occurs rather abruptly above ca. 50 °C and is attributed to phase separation accompanied by gelation. The elastic modulus increases rapidly with temperature, the samples become visibly turbid, and the scattered intensity increases markedly over a wide range of scattering wavevector, q. In contrast, dilute solutions do not gel but give clear evidence of aggregation in the high-temperature regime, consistent with crossing a phase boundary. The SANS structure factor $S(q)$ in the gel state is well described by a sum of two terms, corresponding to two power-law regimes. The lower q regime follows $S(q) \sim q^{-1.8}$ in both the pregel and gel states, consistent with chains intermediate between good and Θ solvent conditions. At higher q the exponent evolves from ca. −2.5 to −4 upon gelation. The latter exponent indicates a sharp boundary between the gel structure and the intervening fluid, consistent with liquid−liquid phase separation that is arrested by gelation.

Introduction

Methylcellulose (MC)—a water-soluble polymer used as a binder or thickener in pharmaceutical, food, and ceramic processing applications—is known to undergo thermoreversible gelation in aqueous solution upon heating.[1−14] Cellulose, the raw material of MC, is hydrophilic, but cellulose fibers contain crystalline ordered regions formed by intra- and intermolecular hydrogen bonds; consequently, cellulose does not dissolve in water. The crystalline fraction depends on the source of cellulose, but when a certain number of the hydroxyl groups are substituted by methoxyl groups, some hydrogen bonds are broken and MC becomes water-soluble. This modification is expressed as the degree of substitution (DS), defined as the number of methoxyl groups divided by the number of glucose units; the structure of cellulose is shown in Figure 1. If the DS is too low, sufficient hydrogen bonds remain that this MC is still insoluble, whereas MC with a high DS is hydrophobic and is also insoluble. Hence, the commercial products usually have an intermediate DS, ca. 1.7−2.0. At low temperatures, water molecules are presumed to form "cagelike" structures to surround the hydrophobic methoxyl groups, causing the MC to become water-soluble.[7,12] Upon heating, these structures distort and break to expose the hydrophobic regions, inducing the formation of aggregates. Thus, the gelation

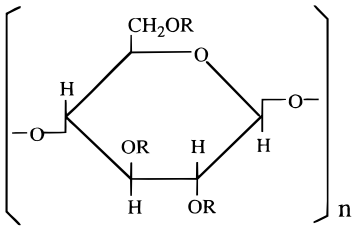

Figure 1. Structure of methylcellulose. R = CH_3 or H.

is a manifestation of the hydrophobic effect, and cosolutes that are readily soluble in water, such as strong electrolytes, depress the gel temperature.[2] Commercial MC is produced by a reaction in which cellulose is exposed to aqueous sodium hydroxide and methyl chloride under mechanical mixing, with the methylation occurring more rapidly in NaOH-rich and/or higher temperature regions. Consequently, it is assumed that the distribution of methyl groups is inhomogeneous along each chain and from chain to chain. MC prepared in a more homogeneous manner, i.e., the reaction carried out in solution, was reported not to undergo gelation for the same average DS.[6] Kato et al. concluded that the crystallites of trimethylglucose units, the most hydrophobic repeat units, act as "cross-linking loci" on heating.[4]

Although the gelation of MC has been studied extensively, a variety of different mechanistic steps have been invoked.[4,7−9,11,13,14] Overall, the experimental evidence favors a two-stage process, in which heating in the lower temperature regime increases interchain clustering due to hydrophobic association, and the actual gelation at higher temperature competes with liquid−liquid phase separation. This interpretation is well-supported by the

§ Department of Chemical Engineering & Materials Science.
† Permanent address: Shinetsu Chemical Co., Ltd., Niigata 942, Japan.
‡ Current address: National Taiwan University of Science and Technology, Taipei, Taiwan.
* To whom correspondence should be addressed.

10.1021/ma990242n CCC: $18.00
Published on Web 10/01/1999

theoretical treatment of Tanaka and co-workers.[15,16] However, the gel formation process has not been explored heretofore in detail by scattering techniques. Consequently, in this paper we examine both the network formation process and the gel structure using light and small-angle neutron scattering, supplemented by rheology and dynamic light scattering.

Experimental Section

Materials. The methylcellulose (MC) used in this work was Metolose SM-4000 from Shinetsu Chemical Co., Ltd.; it was dried overnight under vacuum at 60 °C and then cooled in a desiccator before use.[17] The manufacturer's specifications indicate that the viscosity of a 2 wt % solution was 4.54 Pa s at 20 °C and that the methoxyl content and assay of dry MC were 29.6% and 99.8%, respectively. The DS was measured by the manufacturer to be 1.79, and the density was calculated to be 1.39 g/mL following a literature relation.[18] Spectrophotometric grade H_2O from EM Science was used as received. The MC solutions were prepared by dispersing the polymer into hot water to avoid coagulation. The solutions were then cooled below 5 °C to dissolve MC for at least 1 day prior to use and were stored in a refrigerator.

Rheology. Oscillatory shear measurements of aqueous MC solutions were carried out in a Rheometrics Fluids spectrometer (RFS II) in the cone and plate geometry (cone angle = 0.04 rad, radius = 25 mm). To inhibit dehydration of the solutions, a small amount of low-viscosity silicone oil was placed on the periphery of the solutions. The dynamic storage and loss moduli, G' and G'', were examined as functions of temperature from 20 to 80 °C with a strain amplitude, γ, of 5%, a frequency, ω, of 1 rad/s, and a heating rate of 0.5 °C/min. Isothermal frequency sweeps ($\omega = 0.1-100$ rad/s) on a solution with $c = 0.01$ g/mL were performed at 10 deg intervals between 20 and 70 °C.

Small-Angle Neutron Scattering. The SANS measurements were carried out at the National Institute of Standards and Technology CNRF, on the Exxon/University of Minnesota/NIST 30 m instrument (NG7). Deuterium oxide (D_2O, 99.996 atom % D) from Aldrich was selected as the solvent to provide scattering contrast. The quartz scattering cells had a diameter of 25 mm and a path length of 2 mm. The neutron wavelength was 6 Å with $\Delta\lambda/\lambda = 0.10$, and sample-to-detector distances of 15, 4, and 2.5 m were employed, to extend the accessible q range from approximately 0.003 to 0.25 Å^{-1}. Intensities were corrected for background scattering, detector response, solvent, and cell scattering and placed on an absolute scale via calibration with silica standards (B2 for the 15 m and A5 for the 4 and 2.5 m settings).

Dynamic Light Scattering. An argon ion laser (Lexel model 175, $\lambda_0 = 4880$ Å) was employed with a Malvern spectrometer (PCS100) as the goniometer and scattering apparatus, coupled with a 380-channel multisample time autocorrelator (BI-2030AT) from Brookhaven Instruments. The solutions were filtered through 0.45 μm Millipore filters ($c \leq 0.0025$ g/mL) or 1.2 μm filters ($c \geq 0.005$ g/mL) directly into dust-free scattering cells and sealed. Two sizes of scattering cells, 10 mm o.d. and 5 mm o.d., were selected, depending upon concentration and temperature. The time autocorrelation function of the scattered intensity, $g^{(2)}(q,t)$, obtained from each measurement was analyzed by the inverse Laplace transform program CONTIN.[19] Correlation functions were obtained at 20 and 75 °C for scattering angles, θ, from 30° to 150° in 20° increments and at temperatures from 25 to 70 °C in 5 deg increments, for $\theta = 50°$ and 90°.

Results

The presentation of the results is organized as follows. First, we present light scattering characterization of very dilute MC solutions at low temperature (20 °C), which serves as a reference for the ensuing evolution of structure. The growth of the gel with increasing temperature and concentration, as monitored by rheology, light, and neutron scattering, is then described. Finally, dynamic light scattering measurements over the same range of concentration and temperature are presented.

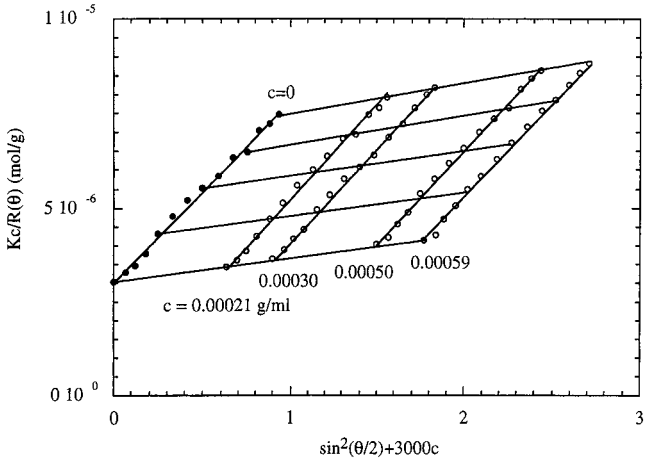

Figure 2. Zimm plot for methylcellulose solutions at 20.0 °C.

Characterization of Methylcellulose in Dilute Solution. The radius of gyration (R_g), second virial coefficient (A_2), and weight-average molecular weight of MC in dilute solution were determined by standard (Zimm) analysis. The scattering intensity from solutions is expressed as

$$\frac{Kc}{R_\theta(q,c)} = \frac{1}{M_w P(q)} + 2A_2 c + \ldots \qquad (1)$$

where $K = 4\pi(dn/dc)^2 n^2/\lambda_0^4 N_A$ with n, λ_0, dn/dc, and N_A being the refractive index of the solvent, the vacuum wavelength of the incident beam, the refractive index increment, and Avogadro's number, respectively. R_θ is the Rayleigh ratio, and $R_{90}(25\ °C) = 35.4 \times 10^{-6}$ and 39.6×10^{-6} cm^{-1} for benzene and toluene, respectively, were employed to calibrate the instrument;[20] q is the standard scattering vector given by $(4\pi n/\lambda_0)\sin(\theta/2)$, and $P(q)$ is the form factor of the chain. The refractive index increment of MC in water was measured using a homemade interferometric differential refractometer with a HeNe laser ($\lambda_0 = 6328$ Å) source. The value of dn/dc at room temperature was 0.137 ± 0.004 mL/g, in good agreement with the value of 0.136 mL/g reported in the literature.[21] This value was used for our SLS experiments without accounting for the difference in λ_0, although the estimated change in dn/dc would be about 4%. The scattering intensities from four solutions with concentrations of 0.000 21, 0.000 30, 0.000 50, and 0.000 59 g/mL were measured at 20 °C, and the resulting Zimm plot is shown in Figure 2. The values of the z-average R_g, A_2, and M_w obtained from this plot were 637 Å, 8.34×10^{-4} mol mL/g^2, and 3.8×10^5 g/mol, respectively. The overlap concentration, c^*, was then estimated as $c^* \approx (A_2 M_w)^{-1} = 0.003$ g/mL. Given this value of M_w, these results for R_g and A_2 are consistent with expectation for dilute solutions of flexible or semiflexible chains in a good solvent.

The Development of Methylcellulose Gels. (a) Rheology. The dynamic moduli were measured during isochronal temperature sweeps from 20 to 80 °C for concentrations from 0.0010 to 0.030 g/mL. The measurement conditions, $\omega = 1$ rad/s and $\gamma = 0.05$, were selected to be as low as possible to avoid destroying the

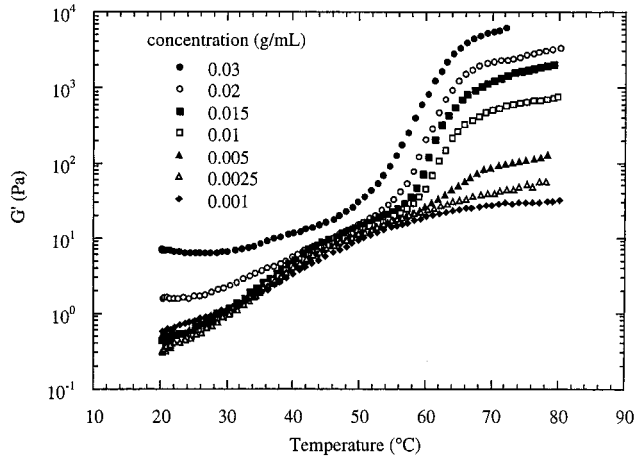

Figure 3. Variation of the dynamic storage modulus G' as a function of temperature at a frequency $\omega = 0.1$rad/s and a strain amplitude $\gamma = 5\%$.

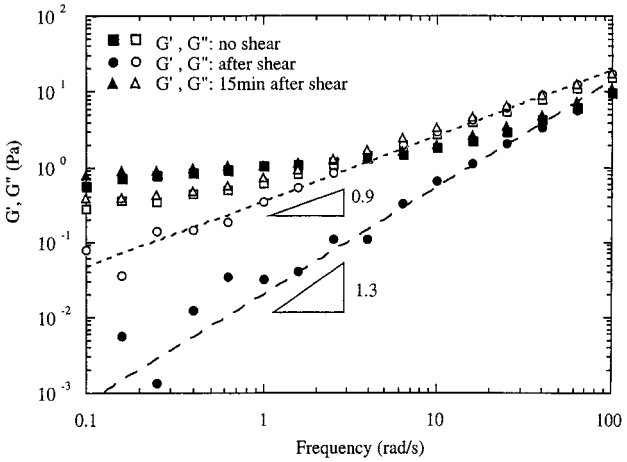

Figure 4. Frequency dependence of G' and G'' for $c = 0.01$ g/mL and $T = 20$ °C under three conditions as indicated in the plot.

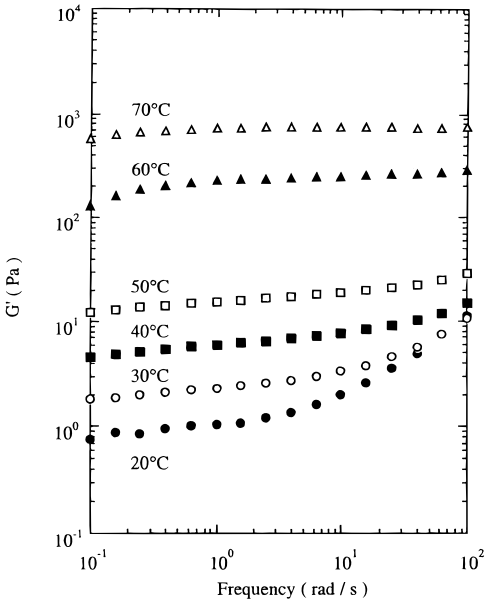

Figure 5. Frequency dependence of G' for $c = 0.01$ g/mL at the indicated temperatures.

aggregates but high enough to obtain accurate results. The heating rate was 0.5 °C/min in all cases. The results for G' for seven concentrations are shown in Figure 3. In all cases G' is a monotonically increasing function of temperature, but the increase proceeds in two stages, in agreement with previous reports.[8,11] The first stage extends from 20 °C with G' increasing slowly up to about 55 °C. For the five lower concentrations, G' is roughly independent of c in this range, whereas for the two higher concentrations, 0.02 and 0.03 g/mL, the modulus is significantly larger even at 20 °C. This may be attributed to the onset of entanglements at these higher concentrations, which correspond to c/c^* values of 7−10. In the second stage, G' increases rapidly with temperature before achieving a near plateau above 65−70 °C. This corresponds to the formation of a strong gel; i.e., the samples no longer flow. Furthermore, these samples became noticeably turbid over the same temperature range. For the two lowest concentrations, with $c/c^* < 1$, gelation does not occur, but for all the semidilute concentrations the gelation is distinct, and the gel modulus increases strongly with concentration. In fact, G' at 70 °C scales as $G' \sim c^{2.3}$ for $c = 0.0050-0.030$ g/mL (not shown), in good agreement with the plateau modulus in concentrated polymer solutions and with expectation for gels swollen in a good solvent.[22] We removed the cone of the rheometer just after the measurements (at ca. 80 °C) and confirmed that gelation had occurred for $c \geq 0.005$ g/mL and that the solutions with $c \leq 0.001$ g/mL remained fluid. For $c = 0.0025$ g/mL, very close to the overlap concentration, a small portion of gel-like solid in solution was observed.

Frequency sweeps were carried out to further examine the structure of MC in aqueous solutions. The $c = 0.01$ g/mL solution was examined from 20 to 70 °C at 10 deg intervals. Figure 4 shows the dynamic moduli at 20 °C under three conditions: as loaded, immediately after manual shearing (i.e., rotation of the fixture), and 15 min after the cessation of shearing. For typical polymer solutions, G' and G'' exhibit a low-frequency terminal response: $G' \sim \omega^2$ and $G'' \sim \omega^1$. For this solution G' and G'' showed apparent exponents of ca. 1.3 and 0.9 immediately after perturbation, which correspond approximately to terminal behavior. The deviations from the expected slopes may be attributed, at least in part, to polydispersity; similar observations have been reported for λ-carrageenan and guar solutions.[23,24] Under the first and last conditions, both moduli were almost flat in the low-frequency regime, suggesting that at equilibrium there is a supermolecular structure maintained by weak reversible association. This corresponds to the regime termed the "clear gel" by other workers.[9] These results suggest, inter alia, that it may be rather difficult to obtain modulus data in the linear viscoelastic limit for these very soft materials. On heating the plateau in G' became wider, and with a significantly enhanced magnitude, as shown in Figure 5. Between 50 and 60 °C, in particular, the modulus increases by an order of magnitude. Above 60 °C G' was flat over the entire accessible frequency, as expected in the gel state.

(b) Light and Neutron Scattering. Whereas the Zimm analysis is appropriate in the dilute regime when $qR_g < 1$, the light scattering intensity in semidilute solutions can be approximated by two relations:

$$\frac{Kc}{R_\theta(q)} \approx \frac{1}{M_{app}}\left(1 + \frac{1}{3}q^2 {R_{g,app}}^2\right) \qquad qR_g < 1 \quad (2a)$$

$$\frac{Kc}{R_\theta(q)} \sim 1 + q^2\xi^2 \qquad q\xi > 1 \tag{2b}$$

where $R_{g,app}$ and ξ represent the apparent radius of gyration and the screening length (or blob size), respectively. Equation 2a reduces to $Kc/R_\theta(0) \approx M_{app}^{-1}$ at $q = 0$, where M_{app} is the apparent molecular weight; eq 2b is the Ornstein−Zernike equation. We examined the solution with $c = 0.0050$ g/mL for temperatures between 20 and 50 °C, i.e., approaching but not achieving the rapid increase in G'. The data are plotted according to eqs 2a and 2b in Figure 6, and two distinct linear regimes are resolved for each temperature. The three parameters thus obtained, M_{app}, $R_{g,app}$, and ξ, are listed in Table 1; the crossover between the two regimes occurs near $q\xi \approx 1$. The variation in M_{app} is consistent with the growth of clusters of increasing mass as the gel point is approached; the rate of increase is much greater at the higher temperatures. This is consistent with the model of Tanaka and Ishida.[15] In contrast, $R_{g,app}$ only increased slightly at 30 and 40 °C and even decreased at 50 °C. This may possibly be understood as reflecting coil shrinkage due to a decrease in effective solvent quality with increasing temperature, as the polymer−polymer interaction becomes more attractive. Consequently, although the number of chains in an average cluster clearly increases, the average dimension varies rather little. (Of course, significantly larger aggregates may scatter at smaller values of q than the instrument can access. It should also be emphasized that a scattering measurement will not provide direct insight into the breadth of the distribution of clusters; recent cryo-TEM measurements on this system indicate a very broad range of associated structures in the pregel regime.[25]) This interpretation is consistent with the results of Kato et al., who measured the osmotic pressure at various temperatures and concluded that water becomes a Θ solvent for their MC at 47 °C.[4] The screening length is independent of temperature within the uncertainty, except for a slight increase at 50 °C. Extensive light scattering measurements at higher temperatures were precluded by multiple scattering.

The structure of the MC solutions and gels was studied using SANS. Typical scattering curves are shown in Figures 7 and 8 for solutions with $c = 0.011$ and 0.019 g/mL, respectively, at various temperatures from 40 to 70 °C; similar behavior was observed for other gel-forming concentrations. The intensity grows markedly upon gelation and particularly at lower q. The strongest increase occurs over the temperature range where G'' also increases the most strongly, i.e., during the second stage of the gelation process. At relatively low q (below ca. 0.01 Å^{-1}) the data follow a power law, with a slope of approximately −1.8, in both low- and high-temperature regimes. Thus, the aspect of the solution structure that gives rise to this power law is unperturbed by the gelation process. This slope implies a self-similar structure with fractal dimension $\Delta \approx 1.8$ or, equivalently, a size vs molecular weight exponent $\nu = {}^5/_9$. This is intermediate between the values of ${}^1/_2$ and ${}^3/_5$ associated with Gaussian and excluded-volume chains. Then there is a high-q region with stronger slope that evolves from ca. −2.5 at low temperatures, i.e., prior to gelation, to ca. −4 in the gel state at 70 °C. (The data beyond ca. 0.1 Å^{-1} should not be considered, because the magnitude of the coherent intensity is 0.01 cm^{-1} or below and thus smaller than the inevitable uncertainty in the incoherent background subtraction.) The former exponent implies a more condensed structure than a Gaussian chain, and the latter is the familiar Porod scaling for a two-phase system with sharp interfaces.

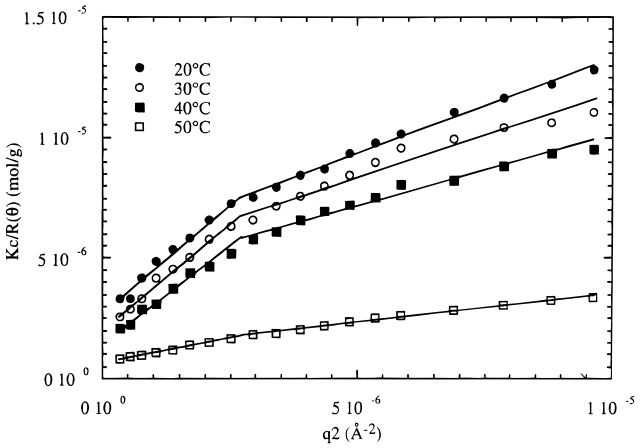

Figure 6. Angle dependence of light scattering for $c = 0.005$ g/mL at the indicated temperatures.

Table 1. Fits of Eq 2 to Light Scattering Data for c = 0.005 g/mL

T (°C)	$R_{g,app}$ (Å)	$M_{app} \times 10^{-3}$	ξ (Å)
20.0	1480	384	382
30.0	1620	494	357
40.0	1670	627	356
50.0	1350	1520	455

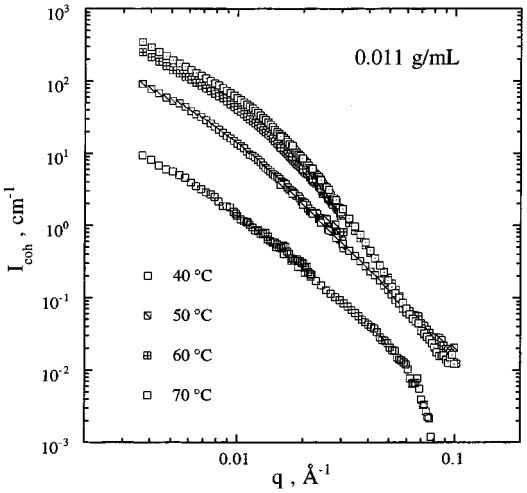

Figure 7. Neutron scattering curves for $c = 0.011$ g/mL at the indicated temperatures.

The structure of the gels (on the length scales probed by SANS) formed at different concentrations is independent of concentration, as shown in Figure 9; here the data at 70 °C are plotted as I/c, with excellent superposition obtained. This result is rather remarkable, as the data extend over almost 2 orders of magnitude in q, more than 4 orders of magnitude in I/c, and over a full order of magnitude in concentration. The smooth curve represents a fit to the data for $c = 0.05$ g/mL, as will be discussed below.

Several workers have considered the structure factor of polymer gels.[22,26−28] The first important issue is to compare the intensity from the gel to that from the semidilute solution from which it was prepared. The reduction in chain mobility implied by gelation should suppress thermal concentration fluctuations, and thus

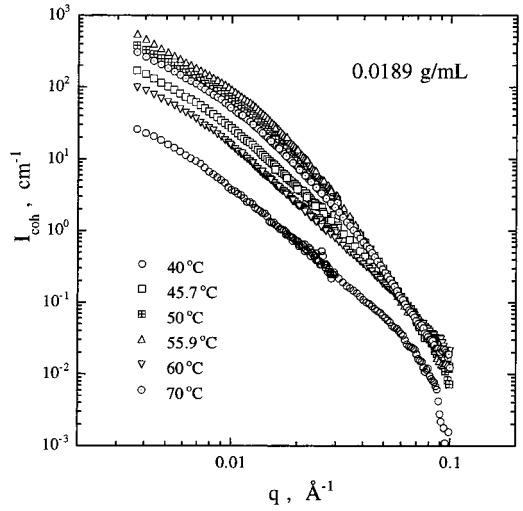

Figure 8. Neutron scattering curves for $c = 0.011$ g/mL at the indicated temperatures.

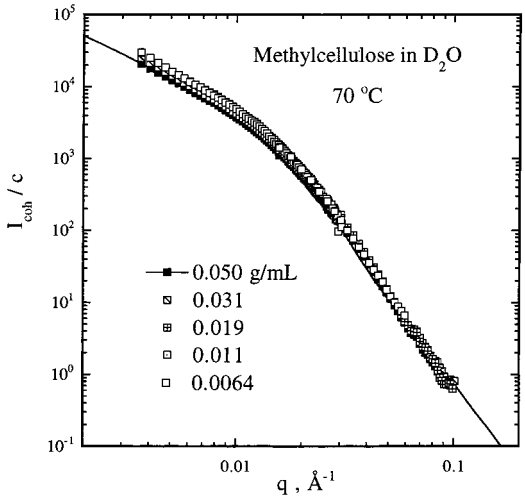

Figure 9. Neutron scattering intensities normalized by concentration for the indicated concentrations, at $T = 70.0$ °C. The smooth curve is a fit to the data for $c = 0.05$ g/mL solution as described in the text and also shown in Figure 10.

the gel intensity should be, if anything, lower than that from the solution, if the gelation process only fixed the instantaneous structure of the solution.[22] However, it is almost universally the case that the scattering from gels is larger than from the equivalent solution, but primarily in the low q regime.[22] The reasons for this remain incompletely understood but almost certainly involve heterogeneity in the spatial distribution of cross-links. A revealing aspect of the data in Figures 7 and 8 is that the intensity increases markedly upon gelation across the accessible q range, with the shape of the curve unchanged in the lower q regime. This can be taken as strong evidence of a phase separation process, which is restricted in space by the concomitant gelation. Thus, it is the effective contrast factor, reflecting the difference in local concentration between polymer-rich and polymer-lean regions, that gives rise to the increased intensity and not a gross change in the structure itself. Phase separation is also indicated by the developing opacity of the gels at high temperature; such opacity is not a routine feature of swollen gels, even if the cross-link distribution is heterogeneous.

The structure of the gels can be placed on a more quantitative basis. Bastide et al. proposed that the gel scattering function could be expressed as

$$I(q) = \frac{a_1}{1 + g(q)q^2\xi_{gel}^2} \tag{3}$$

where a_1 is a constant and ξ_{gel} is the correlation length of the gel, i.e., the blob size between junctions.[26] The function $g(q)$ is given by

$$g(q) = \frac{1}{1 + (q\xi_{gel})^{2-\Delta}} \tag{4}$$

where Δ is the fractal dimension of the so-called "frozen blob" for $q\xi_{gel} > 1$. Subsequently, Coviello et al. introduced a cutoff factor $[1 + g(q)qr_c/\sqrt{2}]\exp(-q^2r_c^2/2)$ into the Bastide equation to avoid incompatibility between this equation and the experimental results at high q.[27,28] Thus, the scattering function becomes

$$I_1(q) = \frac{a_1}{1 + g(q)q^2\xi_{gel}^2}\left(1 + g(q)\frac{qr_c}{\sqrt{2}}\right)\exp\left(\frac{-q^2r_c^2}{2}\right) \tag{5}$$

where r_c is the radius of the cross-linking regions. Coviello et al. applied this equation to the scattering profiles from polysaccharide gels rather successfully.[27] However, eq 5 will not reproduce our data because it does not asymptotically approach the Porod regime ($I \sim q^{-4}$) clearly apparent in the data. Accordingly, we added a Debye−Bueche term of the form[29]

$$I_2(q) = \frac{a_2}{(1 + q^2\rho^2)^2} \tag{6}$$

to eq 5 and used that to fit the data. However, there are more parameters in the combined equations than are really necessary to describe the features in the data. For example, the "Coviello−Bastide" part has an amplitude, a correlation length, the exponent Δ, and the cutoff length scale r_c, whereas the Debye−Bueche term adds a second amplitude and length scale. Therefore, we fixed the exponent Δ to be -1.8, as implied by the data in the higher q regime, and we forced the cutoff length scale and the Debye−Bueche length to be the same, thus reducing the overall fit to two length scales and two amplitudes.

The resulting fit to one set of data in shown in Figure 10, along with the two individual contributions. The fit is satisfactory. The two length scales thus obtained are a correlation length of ca. 1200 Å and a shorter range structural feature of approximately 54 Å. The former length scale is rather imprecise, as it is essentially determined by the first departure of the theoretical curve from its $q = 0$ plateau, and as can be seen in Figure 10, this break does not lie within the range of the actual data. Nevertheless, it is clear that there must be inhomogeneity in the gel structure on length scales comparable to the wavelength of light, or the samples would not become turbid. In contrast, the shorter length scale is very robust, as it corresponds to a clear break in the q dependence of the intensity. It presumably corresponds to the typical thickness of the locally phase-separated structure.

(c) Dynamic Light Scattering. Dynamic light scattering (DLS) was used to confirm the existence of clusters at lower temperatures and to observe the transition from solution to gel upon heating. DLS

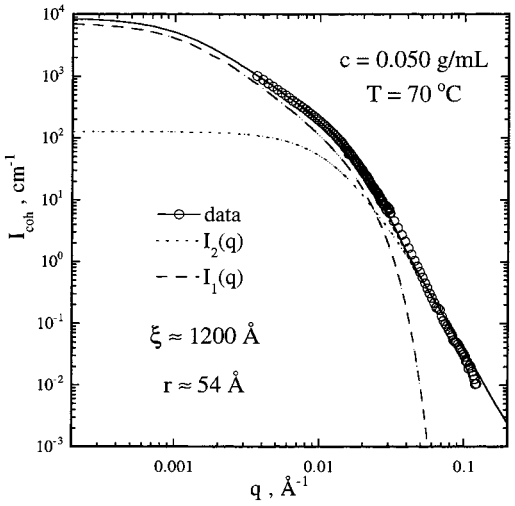

Figure 10. Fit of the combined Bastide−Coviello (I_1) and Debye−Bueche (I_2) structure factors to the neutron scattering data for $c = 0.05$ g/mL and $T = 70$ °C.

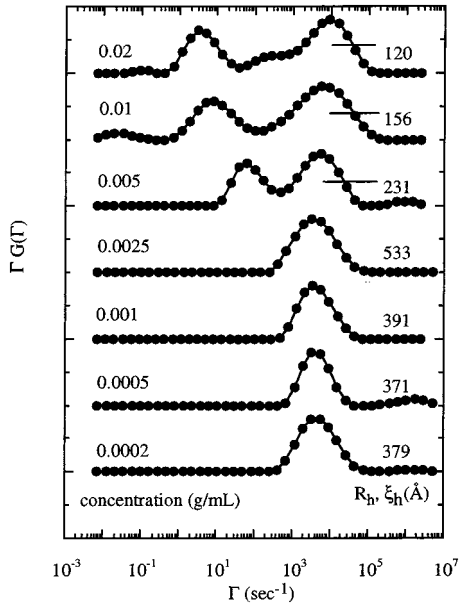

Figure 11. Concentration dependence of the distribution of decay rates at $T = 20$ °C and the associated correlation lengths.

reflects the polymer size and/or correlation length through the dynamics of spontaneous concentration fluctuations. The Laplace inversion routine CONTIN converts the measured intensity autocorrelation function into a distribution of decay rates, $G(\Gamma)$.[19] In cases where a single relaxation mode is observed, or is well-resolved from multiple modes, a mean decay rate Γ is extracted. For diffusive processes, $\Gamma = Dq^2$, and D is related to the hydrodynamic radius in dilute solution, R_h, or the correlation length in semidilute solution, ξ_h, by

$$D = \frac{kT}{6\pi\eta_s R_h} \quad \text{or} \quad \frac{kT}{6\pi\eta_s \xi_h} \tag{7}$$

where k and η_s are the Boltzmann constant and solvent viscosity, respectively.

The distribution of decay rates at 20 °C for $c = 0.00020-0.020$ g/mL are shown in Figure 11 in the equal area format ($\Gamma G(\Gamma)$ vs Γ). For dilute solutions, $c \leq 0.0025$ g/mL, only one mode was observed and was

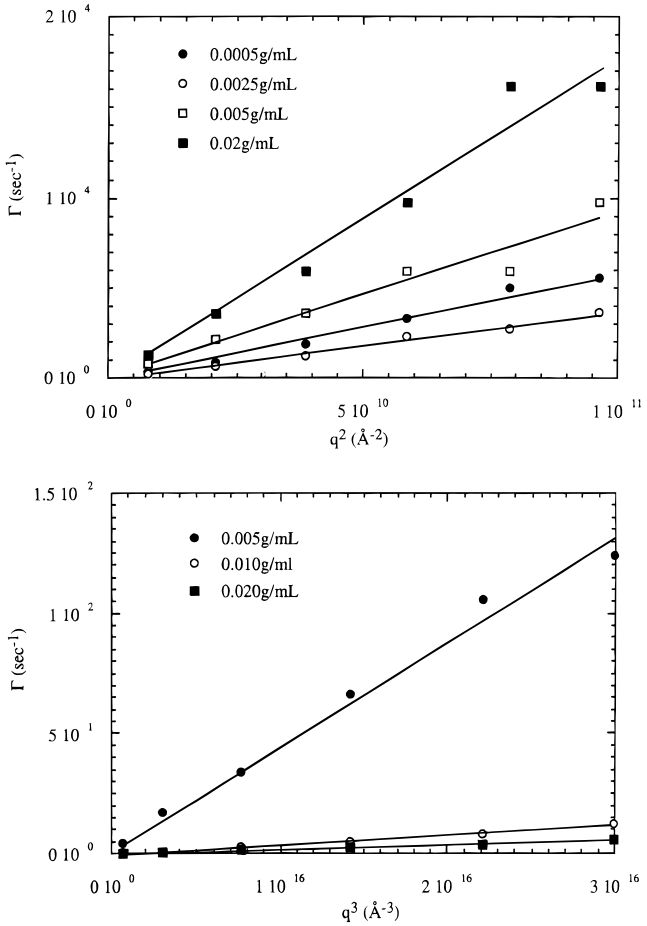

Figure 12. Wavevector dependence of the decay rate for (a, top) the fast mode and (b, bottom) the slow mode in Figure 11.

attributed to chain diffusion. The resulting values of the hydrodynamic radius (380 ± 10 Å) were independent of concentration for $c = 0.0002-0.001$ g/mL, and thus $R_g/R_h \approx 1.7$. This value is consistent with results on (possibly polydisperse) flexible polymers in solution.[30] In the semidilute regime, two modes were resolved. The faster one corresponds to the standard cooperative diffusion process, with the corresponding diffusivity increasing with concentration. The diffusive character of the (dilute) translational and (semidilute) cooperative modes is established by the proportionality of Γ to q^2, as illustrated in Figure 12a. The slower mode that emerges in semidilute solutions is attributed to clusters, as suggested by light scattering and rheology. For this mode, Γ was approximately proportional to q^3 (shown in Figure 12b), which is indicative of internal modes of a flexible structure with typical dimension larger than q^{-1}.

The $\Gamma G(\Gamma)$ for solutions with $c = 0.0005$ and 0.005 g/mL upon heating from 20 to 75 °C are shown in Figures 13 and 14, respectively. In this case the horizontal axis Γ was normalized by the solvent viscosity at each temperature, to aid in comparison. For the dilute solution, 0.0005 g/mL, the single mode is essentially constant from 20 to 50 °C (with $R_h \approx 380$ Å) and then slows rather abruptly from 55 to 60 °C. This suggests that the isolated MC chains begin to aggregate near 55 °C, consistent with the onset of phase separation, but the concentration is too low to form a gel. Above 60 °C the mean Γ was also roughly constant, scaled linearly with q^2, and gave a hydrodynamic radius of ca. 3400 Å

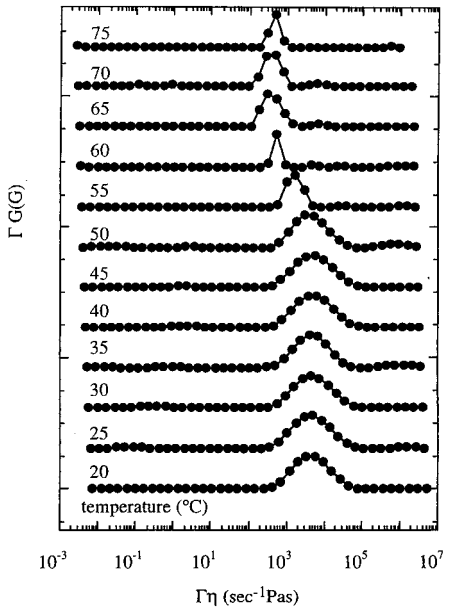

Figure 13. Temperature dependence of the distribution of decay rates for a nongelling solution with $c = 0.0005$ g/mL.

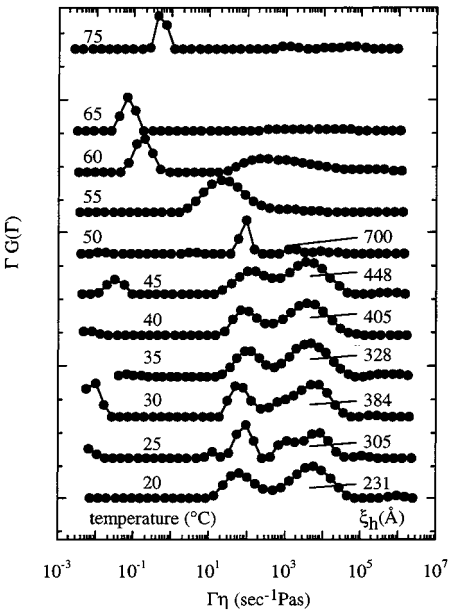

Figure 14. Temperature dependence of the distribution of decay rates for a gelling solution with $c = 0.005$ g/mL and the associated correlation lengths.

at 75 °C. The solution with $c = 0.001$ g/mL (data not shown) gave equivalent results. For the solution with $c = 0.005$ g/mL, which formed a strong gel at high temperature, the decay rate distributions were more complicated as illustrated in Figure 14. The two modes evident at 20 °C persist up to 45 °C, but beyond that the slow mode dominates the scattering intensity and moves to much lower frequencies. This "extra-slow" mode was observed in the 0.0025 g/mL solution and all solutions in the semidilute concentration regime in the gel state.

Discussion

As noted in the Introduction, there have been several proposals for the gelation mechanism in aqueous MC solutions. Most acknowledge a two-stage process, as exemplified by the rheological signatures in Figure 3, but differ in the identity of the two stages. For example, Haque and Morris suggest that at low temperatures residual crystallinity causes the chains to be dispersed in bundles, which gradually disintegrate (stage I) before hydrophobic association leads to gelation (stage II).[7] Others have emphasized the role of phase separation, especially with reference to stage II, and have mapped out an LCST phase diagram for MC/water.[9,10] Crystallinity plays a role, as indicated by two distinct peaks in DSC measurements.[4,7,11,14] Finally, Kato et al. have proposed that stage I is driven by aggregation of the most hydrophobic domains, presumably those glucose residues that are trisubstituted, whereas stage II reflects association of less hydrophobic groups (di- and monosubstituted).[4] These various possible mechanisms are not all mutually exclusive, of course. We interpret our results as indicating that stage I is caused by hydrophobic association, leading to a broad distribution of aggregate shapes and sizes, and that stage II is gelation intermingled with phase separation. The basis for this interpretation is detailed below.

The Zimm plot in Figure 2 is strong evidence for the existence of molecularly dissolved chains at low temperature, in very dilute solution. Similarly, this conclusion is supported by the dynamic light scattering results in the dilute regime. Although we cannot exclude the possibility of some small quantity of crystalline aggregates, as envisioned by Haque and Morris,[7] they certainly cannot be a significant component. For semidilute solutions at low temperature, there is some intermolecular association, as evidenced by the shear-dependent rheological properties (Figure 4) and the slow mode in the dynamic light scattering spectrum. Previous workers have taken the fact that $G' > G''$ at low frequency in this regime as evidence of a "weak gel" state.[9] Phenomenologically, our rheology results are quite consistent with theirs, but whether the use of the term "gel" is appropriate will depend on its definition.

All of our results are consistent with the first stage of gelation corresponding to the growth of clusters or aggregates in semidilute solution. The light scattering at low q clearly indicates an increase in the average cluster molecular weight, whereas the neutron scattering suggests that there are no particular changes in structure at an intermediate length scale (where the fractal dimension is about 1.8). The elastic modulus increases steadily, indicative of an increase in the density of cross-linking sites. The dynamic light scattering properties do not change much in this regime, as the average mesh size is dependent on concentration but not temperature.

Similarly, the data are all consistent with the second stage of gelation corresponding to liquid−liquid phase separation that is arrested in space by the associations among chains. The sharp increase in modulus indicates a similar increase in the cross-link density, but if this were solely due to hydrophobic association, there is no mechanism for the development of turbidity. For example, if the first stage were viewed as a semidilute solution with a certain temperature-dependent degree of interchain association and the second stage an enhancement of the number of associations due to the hydrophobic effect, then the resulting gel should be roughly as homogeneous as the precursor solution. The turbidity, on the other hand, is clear evidence of concentration inhomogeneities on the length scale of the wavelength of light, which are simply not present during

the first stage. Phase separation provides a natural mechanism for the growth of such inhomogeneities. The SANS results also support this interpretation, in two ways. First, the strong increase in intensity with temperature is not consistent with an increased cross-linking of an otherwise homogeneous semidilute solution; in such a scenario the intensity should be constant or even decrease. Second, the emergence of a clear Porod regime at high q suggests the formation of two phases with relatively sharp interfaces; conversely, such a Porod regime is not observed in other gelation processes. As noted before, this overall picture is quite consistent with the theoretical description of network formation by hydrophobic association developed by Tanaka and co-workers.[15,16]

Summary

The thermoreversible gelation of a commercial methylcellulose sample in water was examined using a combination of rheology, light scattering, SANS, and DLS. Solutions with concentrations exceeding the coil overlap condition ($c^* \approx 0.003$ g/mL) formed gels upon heating, whereas dilute solutions did not. The gelation proceeded in two stages, as noted by previous workers. The first stage was attributed to hydrophobic association leading to cluster formation, whereas the second stage corresponded to phase separation accompanied by gelation; the crossover temperature between the two stages depended on concentration but was in the vicinity of 50 °C. Very dilute solutions showed no evidence of hydrophobic association but did exhibit aggregation above 50 °C.

At the lowest temperature examined, 20 °C, static and dynamic light scattering from dilute solutions indicated that the weight-average molecular weight was 3.8×10^5 g/mol and that the radius of gyration and hydrodynamic radius were 637 and 380 Å, respectively. Semidilute solutions at the same temperature showed evidence of a weak supermolecular association, or clustering, in the dynamic shear moduli and in light scattering. As the temperature was increased, this clustering was significantly enhanced, as evidenced by growth of the elastic modulus and the scattered intensity (both light and SANS). However, the overall structure of the solutions did not change much over the interval 20−50 °C, as suggested by the relative invariance of the apparent cluster size, the static and dynamic correlation lengths, and the shape of the SANS structure factor.

Above ca. 50 °C, the elastic modulus increased sharply, the samples became turbid and solidlike, and the SANS intensity increased further. In the high q regime, the SANS structure factor developed a significant regime of Porod's law behavior, indicative of strong local segregation of polymer-rich and polymer-lean regions. These observations are all consistent with phase separation accompanied by gelation. The SANS structure factor in the gel state was independent of concentration and could be well described by a sum of two terms. The first, which was designed to fit the lower q data, was adapted from that proposed by Coviello et al.[27] and Bastide et al.,[26] and the second was of the Debye−Bueche form,[29] which recovers the Porod scaling at high q. The domain length scale associated with the Debye−Bueche term was approximately 50 Å.

Acknowledgment. We acknowledge Dr. Z. Liu for assistance with the light scattering measurements, Professor W. Miller for the generous loan of his rheometer, and Professor Y. Talmon for helpful discussions.

References and Notes

(1) Heymann, E. *Trans. Faraday Soc.* **1935**, *31*, 846.
(2) Savage, A. B. *Ind. Eng. Chem.* **1957**, *49*, 99.
(3) Sarkar, N. *J. Appl. Polym. Sci.* **1979**, *24*, 1073.
(4) Kato, T.; Yokoyama, M.; Takahashi, A. *Colloid Polym. Sci.* **1978**, *256*, 15.
(5) Takahashi, S.; Fujimoto, T.; Miyamoto, T.; Inagaki, H. *J. Polym. Sci., Polym. Chem. Ed.* **1987**, *25*, 987.
(6) Ibbett, R. N.; Phillip, K.; Price, M. *Polymer* **1992**, *33*, 4087.
(7) Haque, A.; Morris, E. R. *Carbohydr. Polym.* **1993**, *22*, 161.
(8) Hirrien, M.; Desbrières, J.; Rinaudo, M. *Carbohydr. Polym.* **1996**, *31*, 243.
(9) Hirrien, M.; Chevillard, C.; Desbrières, J.; Axelos, M. A. V.; Rinaudo, M. *Polymer* **1998**, *39*, 6251.
(10) Chevillard, C.; Axelos, M. A. V. *Colloid Polym. Sci.* **1997**, *275*, 537.
(11) Nishinari, K.; Hofmann, K. E.; Moritaka, H.; Kohyama, K.; Nishinari, N. *Macromol. Chem. Phys.* **1997**, *198*, 1217.
(12) Sarkar, N. *Carbohydr. Polym.* **1995**, *26*, 195.
(13) Vigouret, M.; Rinaudo, M.; Desbrières, J. *J. Chim. Phys.* **1996**, *93*, 858.
(14) Yuguchi, Y.; Urakawa, H.; Kitamura, S.; Ohno, S.; Kajiwara, K. *Food Hydrocolloids* **1995**, *9*, 173.
(15) Tanaka, F.; Ishida, M. *J. Chem. Soc., Faraday Trans.* **1995**, *91*, 2663.
(16) Tanaka, F. *Adv. Colloid Interface Sci.* **1996**, *63*, 23.
(17) The experimental evidence presented herein suggests that the properties of this particular sample are broadly comparable to those from other commercial sources.
(18) Uda, K.; Meyerhoff, G. *Makromol. Chem.* **1961**, *47*, 168.
(19) Provencher, S. W. *Comput. Phys. Commun.* **1982**, *27*, 229.
(20) Bender, T. M.; Lewis, R. J.; Pecora, R. *Macromolecules* **1986**, *19*, 244.
(21) Spurlin, H. M. *J. Am. Chem. Soc.* **1939**, *61*, 2222.
(22) Bastide, J.; Candau, S. J. *Structure of Gels as Investigated by Means of Static Scattering Techniques*; Cohen-Addad, J. P., Ed.; J. Wiley & Sons: Chichester, UK, 1996.
(23) Morris, E. R. In *Gums and Stabilizers for the Food Industry*; Phillips, G. O., Wedlock, D. J., Williams, P. A., Eds.; Pergamon: Oxford, 1984; Vol. 2.
(24) Clark, A. H.; Ross-Murphy, S. B. *Adv. Polym. Sci.* **1987**, *83*, 57.
(25) Goldraich, M.; Gottlieb, M.; Talmon, Y., unpublished results.
(26) Bastide, J.; Leibler, L.; Prost, J. *Macromolecules* **1990**, *23*, 1821.
(27) Coviello, T.; Burchard, W.; Geissler, E.; Maier, D. *Macromolecules* **1997**, *30*, 2008.
(28) Horkay, F.; Hecht, A.-M.; Mallam, S.; Geissler, E.; Rennie, A. R. *Macromolecules* **1991**, *24*, 2896.
(29) Debye, P.; Bueche, A. M. *J. Appl. Phys.* **1949**, *20*, 518.
(30) Burchard, W. In *Light Scattering: Principles and Development*; Brown, W., Ed.; Clarendon Press: Oxford, 1996.

MA990242N